



## Routing and Geochemical Properties of Clastic Sediments in Southwestern Iran

Amir Jokar\*, Nader Kohansal Ghadimvand, Davood Jahani and Mahdi Mashal

Department of Geology, Faculty of Basic Sciences, North Tehran Branch, Islamic Azad University, Tehran, Iran

\*Corresponding author: Amir Jokar, Department of Geology, Faculty of Basic Sciences, North Tehran Branch, Islamic Azad University, Tehran, Iran; E-mail: amir\_jokar\_12@yahoo.com

Received date: 03 December, 2021, Manuscript No. JSPH-21-34777;

Editor assigned date: 06 December, 2021, PreQC No. JSPH-21-34777 (PQ);

Reviewed date: 20 December, 2021, QC No JSPH-21-34777;

Revised date: 27 December, 2021, Manuscript No. JSPH-21-34777 (R);

Published date: 03 January, 2022, DOI:10.4172/jsph.1000122

### Abstract

The Khuzestan plain is located in the southwest of Iran in the Khuzestan province and southwest of the Zagros Mountains. It is a part of the Arabian platform and has a completely sedimentary rock lithology. As one of the most important oil regions of Iran and the Middle East, the plain is of great importance in the geochemical and environmental studies. These studies aim to examine 276 sedimentary samples from different parts of this plain. Initially, the basic sedimentary properties of the samples are studied, especially in terms of grading and particle size changes. Then, the detailed geochemical analysis of the sediments is performed to determine all sediment properties, including the routing, paleoclimatology, and environmental characteristics of the sediments. The results of granulometric studies indicate that the sediments are mainly of silt and clay dimensions, and the particles of sand and gravel dimensions are less frequent in the study areas. Investigating the geochemical properties of the sediments indicates that the most frequent constituent oxides in the study area are CaO, SiO<sub>2</sub> and Al<sub>2</sub>O<sub>3</sub>, respectively. Also, according to the studies, the most frequent sub-elements in the study areas are Ti, Zr, V, Ce and La, respectively. The classification of the sediments based on the geochemical indicators shows that the sediments are mainly in the range of greywacke and ferruginous shales. In addition, the paleoclimatological studies indicate the arid to semi-arid climate conditions in the sediment source area. The tectonic setting studies in the area based on the geochemical properties of the sediments indicate the tectonic settings of continental island arc and active continental margin. Also, the routing of the sediments indicates the mainly felsic and sometimes mafic source of the mentioned sediments. The study of environmental contamination in the study areas indicates that elements Ni, Cr and Zn are the most frequent heavy metals in the sediments.

**Keywords:** Khuzestan plain; Geo chemical studies; Clastic sediments; Environmental studies

### Introduction

The Khuzestan Plain is part of the Mesopotamian Plain and is located southwest of Zagros. It is the geological extension of the northern front of the Arabian platform. This plain is simple in terms of

structure and is limited to very gentle folds with a north-south axis, which follows the general fold axis of the Arabian platform. The plain surface is relatively smooth covered by alluvial sediments, which is composed of coarse-grained alluvial sediments in the northern parts and fine-grained sediments in the southern parts. With an area of about 64,236 square kilometers, Khuzestan province is located in southwestern Iran. About 60% of this province (especially in the western and southern parts) is covered with quaternary sediments [1].

The sediments of this plain mainly include silt, clay, sand, gravel, and evaporates (gypsum and anhydrite). These studies aim to examine the geochemical properties of the sediments due to the high importance of studying the mentioned sediments because of various mineral and environmental uses (including the presence of pollution caused by fine dust and pollution of industrial and mineral sectors).

### Geology of Area

The study area is located in southwestern Iran in Khuzestan province and is part of the large Zagros fold belt (Figure 1).



Figure 1: Location image of Khuzestan plain.

About 60% of Khuzestan province consists of plain and foothill areas where foothills and slopes overlook the northern plains [2]. Therefore, the general slope of the Khuzestan plain is north to south and is gentle due to the smooth land [3]. The maximum elevation in the northern plains of the province is 150m, and the minimum elevation in the Persian Gulf coast is zero [4].

Although the Zagros basin has folded during the upper pliocene due to the late alpine orogenic phase, the Khuzestan plain has slightly folded and has become a subsided area due to the bedrock stability. Based on the geological maps and surface and subsurface studies conducted in the area, it can be confidently stated that the area under study is located on the alluvial sediments of the present era consisting of fine grained clay and silt and medium-grained sand sediments. The thickness of the sediments gradually increases from north to south towards the coast of the Persian Gulf.

## Research Method

The studies conducted in this study are divided into two categories: Field and laboratory studies (Figure 2). For the field studies, after performing basic studies, including the collection of library data and related literature, the desired points were identified through satellite images, and the necessary measures were then taken for field visits. In the field studies, in addition to imaging and examining the sedimentary properties of the area 276 samples were collected for the granulometric and geochemical studies.

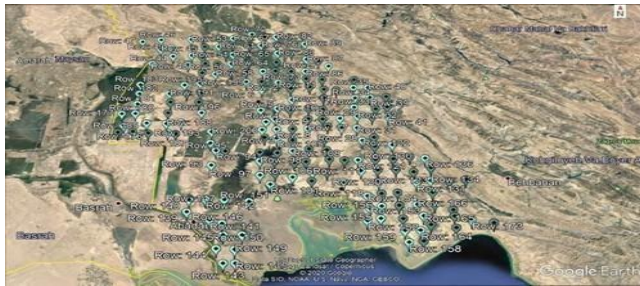


**Figure 2:** Image of location of surveyed points.

Sample No	X	Y	Gravell%	Sand%	Silt%	Clay%
Kh-2	30°38'46.7"N	48° 03'01.32"E	0/29	06/1	75/07	18/53
Kh-5	30°57'20.50"N	48° 04'16.0"E	0/36	3/75	83/91	11/99
Kh-11	30°32'57.7"N	48°19'04.1"E	0/23	02/6	87/54	10/16
Kh-13	30°43'51.9"N	48°15'27.8"E	0/35	5/22	82/35	12/9
Kh-14	30°49'8.96"N	48°16'1.56"E	0/13	13/92	69/11	16/85
Kh-16	30°43'17.7"N	48°22'41.6"E	0/49	7/17	87/82	3/53
Kh-17	30°50'22.1"N	48°24'06.8"E	0	03/7	84/71	12/21
Kh-26	30°56'17.7"N	48°43'00.8"E	0	22/55	68/85	08/6
Kh-27	30°33'24.2"N	48°45'18.9"E	0	0/64	82/77	16/59
Kh-31	30°55'41.74"N	48°47'46.0"E	0/12	10/91	76/79	12/19
Kh-33	30°36'23.9"N	48°53'41.3"E	01/2	6/58	78/48	13/74
Kh-34	30°43'14.0"N	48°54'31.1"E	0/36	03/11	82/73	13/8
Kh-36	30°54'24.22"N	48°53'56.9"E	0/69	8/73	80/52	10/5
Kh-37	30°34'19.0"N	49° 00'48.8"E	0	11/59	74/35	14/6
Kh-38	30°38'24.3"N	49° 01'17.2"E	0/65	09/3	74/88	15/45
Kh-43	30°38'13.87"N	49°6'45.0"E	0	16/91	71/71	11/38
Kh-45	30°49'00.1"N	49°07'01.3"E	0/26	7/51	79/23	13
Kh-46	30°54'05.1"N	49°06'22.0"E	0/2	1/17	84/33	14/3
Kh-47	30°33'25.3"N	49°12'37.3"E	0	08/7	79/43	12/5

**Table 1:** Some grading results of studied samples and geographical location of samples.

The mentioned samples were subjected to XRD, XRF and ICP MASS geochemical analyses in the laboratory studies after the separation and grading by standard sieves. In addition, Scanning Electron Microscopy (SEM) was used formore detailed mineralogical studies. The results of the experiments were analyzed and carefully interpreted to investigate the sedimentary properties of the samples.

## Discussion

### Granulometry

Granulometric is the measurement of particle diameters and the identification of the density ratios. In this section, the results obtained from the grain analysis and relevant statistical data are presented and the results are then discussed (Table 1).

### Geochemical studies

The geochemical studies performed on the samples by XRD, XRF, ICP MASS studies presented extensive results, which are examined in the following section.

**Study of Oxides:** The results of analyzing the samples in the study areas show that CaO, SiO<sub>2</sub> and Al<sub>2</sub>O<sub>3</sub> are the most frequent oxides available and the least oxides in the areas are P<sub>2</sub>O<sub>5</sub>, SrO, TiO<sub>2</sub> and K<sub>2</sub>O (Table 2, Figure 3).

Sample No	Elements									
	Al <sub>2</sub> O <sub>3</sub>	SiO <sub>2</sub>	Fe <sub>2</sub> O <sub>3</sub>	CaO	MgO	Na <sub>2</sub> O	K <sub>2</sub> O	TiO <sub>2</sub>	P <sub>2</sub> O <sub>5</sub>	SrO
Kh-2	7.48	34.25	5.56	28.96	6.58	3.14	0.55	0.5778	0.1741	0.105
Kh-3	7.63	35.63	6.43	30.5	7.26	2.53	0.51	0.5955	0.168	0.165
Kh-4	10.77	30.23	5.1	24.3	3.56	3.47	0.56	0.46	0.1729	0.081
Kh-5	8.78	19.14	6.59	34.2	4.34	2.77	0.55	0.6891	0.2121	0.075
Kh-8	8.76	18.22	7.16	36.2	6.33	1.65	0.62	0.616	0.192	0.086
Kh-11	8.08	20.25	6.43	37.49	4.51	1.64	0.51	0.5047	0.1869	0.071
Kh-12	8.25	19.55	6.34	33.72	5.9	1.32	0.5	0.5454	0.1868	0.093
Kh-13	7.02	45.88	5.73	31.9	5.32	3.49	0.48	0.5308	0.1641	0.062
Kh-14	6.38	8.34	4.56	38.75	4.29	1.76	0.42	0.5209	0.1965	0.068
Kh-16	6.4	7.43	5.99	41.97	5.86	1.42	0.45	0.6262	0.2013	0.07
Kh-17	8.82	8.44	6.29	35.95	4.17	1.05	0.51	0.6402	0.2098	0.063
Kh-18	8.1	8.19	5.67	40.99	3.88	0.55	0.48	0.6157	0.2407	0.071
Kh-20	7.46	22.95	5.24	38.89	4.19	0.7	0.43	0.5508	0.2194	0.066
Kh-23	8.63	7.41	5.99	39.87	4.69	1.52	0.57	0.4864	0.1835	0.128
Kh-24	6.99	6.01	4.23	38.47	5.35	1.63	0.45	0.426	0.2003	0.133
Kh-25	6.34	8.11	4.64	41.97	4.95	2.99	0.44	0.418	0.2158	0.121
Kh-26	6.95	9.06	6.34	41.97	5.65	1.56	0.44	0.6223	0.2265	0.096
Kh-27	6.74	8.33	5.73	38.75	6.11	3.14	0.53	0.5239	0.186	0.086
Kh-28	5.59	8.71	3.51	41.97	4.02	1.29	0.42	0.3853	0.1883	0.142
Kh-29	5.19	9.22	3.67	41.97	6.06	1.69	0.4	0.4305	0.2067	0.115
Kh-30	6.66	8.92	5.41	41.97	6.23	3.03	0.48	0.4911	0.2168	0.128
Kh-31	8.2	8.26	6.66	41.97	6.01	2.41	0.48	0.6437	0.2475	0.095

**Table 2:** Some results from geochemical study of samples.



**Figure 3:** Average percentage of oxides in studied samples; (A) Pie chart and (B) Bar chart.

**Sub-Elements:** After reviewing the results from the study of sub-elements in the areas, the most frequent sub-element is Titanium (Ti) followed by Zr, V, Ce, La, respectively. Figure 4 shows the average frequency percentage of sub-elements in ppm (Table 3 and Table 4).

Sample No	Elements							
	Ce	La	Nb	Sc	Ta	Th	Y	Ti
Kh-2	20.4	9.69	5.84	7.78	0.35	2.48	7.18	3464
Kh-3	19.2	9.52	5.92	7.7	0.5	2.79	7.62	3570
Kh-4	19.8	9.86	5.4	7.51	0.36	2.9	7.21	2758

Kh-5	25.7	12.4	8.68	8.36	0.77	3.09	9.46	4131
Kh-8	24.9	12.8	7.31	8.91	0.74	3.37	9.12	3693
Kh-11	18.7	9.56	5.81	6.55	0.34	2.61	7.27	3026
Kh-12	20.6	10	6.53	7.07	0.6	2.88	7.53	3270
Kh-13	17.2	9.06	5.27	5.76	0.27	2.28	6.16	3182
Kh-14	22.1	11.1	5.92	5.94	0.35	2.7	8	3123
Kh-16	22.7	12.2	8.11	6.64	0.36	3.07	8.93	3754
Kh-17	32	16.7	11.2	10.4	0.68	4.33	16.3	3838
Kh-18	33.6	17.9	12.2	9.33	0.75	3.96	16.2	3691
Kh-20	38	19.5	12.9	10.5	1.05	4.79	17.6	3302
Kh-23	30.3	16.5	10.3	9.67	0.94	4.31	14	2916
Kh-24	26.1	14.4	8.72	8	0.38	3.65	11.7	2554
Kh-25	25.6	13.6	8.35	7.45	0.42	3.42	12.2	2506
Kh-26	37.7	20.1	11.8	11.4	0.63	4.91	18.2	3731
Kh-27	29.2	16.7	11.1	11.2	0.52	4.14	14.8	3141
Kh-28	23	12.5	6.33	6.34	0.05	3.09	11.5	2310
Kh-29	25.7	13.7	7.33	6.04	0.19	3.11	10.8	2581
Kh-30	17.9	10.2	5.71	4.94	0.32	2.4	7.84	2944
Kh-31	32.4	18.9	8.92	8.65	0.48	3.83	13.8	3859
Kh-33	15.8	9.62	5.25	5.23	0.23	2.09	7.41	2629
Kh-34	23.1	13.5	7.07	6.01	0.35	3.13	9.03	3041
Kh-35	21.9	13.6	7.37	7.12	0.42	3.34	10.7	2992

**Table 3:** Results from study of rare earth elements in area.

Sam ple No	Elements																
	Ce	Dy	Er	Eu	Gd	Ho	La	Lu	Nd	Pr	Sc	Sm	Ta	Tb	Tm	Y	Cd
KH-2	20.4	1.19	1.1	0.51	1.65	0.3	9.7	0.08	7.74	2.4	7.78	1.58	0.35	0.26	0.13	7.2	<5.00
KH-3	19.2	1.31	1.2	0.52	1.73	0.36	9.5	0.07	8.95	2.1	7.7	1.59	0.5	0.31	0.16	7.6	<5.00
KH-4	19.8	1.34	1.3	0.48	1.59	0.33	9.9	0.08	9.2	2.3	7.51	1.51	0.36	0.29	0.17	7.2	<5.00
KH-5	25.7	1.56	1.8	0.59	2.38	0.42	12	0.09	10	3	8.36	1.91	0.77	0.37	0.18	9.5	<5.00
KH-8	24.9	1.67	1.6	0.7	2.07	0.45	13	0.1	9.71	2.9	8.91	1.84	0.74	0.41	0.2	9.1	<5.00
KH-11	18.7	1.18	1.1	0.45	1.59	0.28	9.6	0.07	8.67	2.2	6.55	1.53	0.34	0.26	0.14	7.3	<5.00
KH-12	20.6	1.29	1.3	0.61	1.86	0.35	10	0.09	9.26	2.7	7.07	1.66	0.6	0.29	0.16	7.5	<5.00
KH-13	17.2	1.05	0.9	0.46	1.52	0.28	9.1	0.06	7.35	2.1	5.76	1.34	0.27	0.27	0.14	6.2	<5.00

KH-14	22.1	1.45	1.2	0.52	1.91	0.36	11	0.08	10.6	2.9	5.94	1.79	0.35	0.34	0.15	8	<5.00
KH-16	22.7	1.51	1.1	0.49	1.88	0.36	12	0.1	10.9	3	6.64	1.82	0.36	0.32	0.16	8.9	<5.00
KH-17	32	2.96	1.8	0.66	3.08	0.56	17	0.14	14.2	4.2	10.4	2.65	0.68	0.48	0.25	16	<5.00
KH-18	33.6	2.46	1.8	0.65	2.74	0.54	18	0.15	14.5	3.9	9.33	2.82	0.75	0.48	0.24	16	<5.00
KH-20	38	2.91	2.1	0.77	3.45	0.64	20	0.18	16.2	5.4	10.5	3.33	1.05	0.52	0.32	18	<5.00
KH-23	30.3	2.25	1.6	0.57	2.48	0.45	17	0.15	13	3.9	9.67	2.5	0.94	0.37	0.24	14	<5.00
KH-24	26.1	2.17	1.7	0.53	2.27	0.41	14	0.1	10.7	3.4	8	2.2	0.38	0.33	0.19	12	<5.00
KH-25	25.6	1.98	1.5	0.48	2.19	0.39	14	0.11	9.9	3.4	7.45	2.15	0.42	0.3	0.22	12	<5.00
KH-26	37.7	3.08	2.3	0.86	3.26	0.73	20	0.2	16.9	4.7	11.4	3.53	0.63	0.54	0.31	18	<5.00
KH-27	29.2	2.45	1.7	0.58	2.51	0.5	17	0.13	12	4	11.2	2.36	0.52	0.43	0.22	15	<5.00
KH-28	23	2.02	1.3	0.62	1.98	0.41	13	0.1	10.7	3.2	6.34	2.21	0.05	0.34	0.18	12	<5.00
KH-29	25.7	1.91	1.2	0.51	2.15	0.38	14	0.12	11.8	3.7	6.04	2.32	0.19	0.36	0.17	11	<5.00
KH-30	17.9	1.15	0.9	0.28	1.26	0.23	10	0.07	7.95	2.8	4.94	1.32	0.32	0.17	0.13	7.8	<5.00
KH-31	32.4	2.27	1.7	0.58	2.87	0.5	19	0.17	13.9	4.6	8.65	2.48	0.48	0.41	0.23	14	<5.00
KH-33	15.8	0.96	0.8	0.3	1.06	0.24	9.6	0.07	7.29	2.4	5.23	1.22	0.23	0.17	0.12	7.4	<5.00
KH-34	23.1	1.45	1.2	0.4	1.67	0.36	14	0.1	10	3.3	6.01	1.72	0.35	0.28	0.16	9	<5.00
KH-35	21.9	1.55	1.1	0.41	1.69	0.34	14	0.12	11.2	3.8	7.12	1.68	0.42	0.26	0.17	11	<5.00
KH-36	19	1.23	1	0.36	1.43	0.35	12	0.08	9.31	2.6	6.31	1.49	0.55	0.22	0.15	9.3	<5.00
KH-37	20.7	1.52	1.1	0.53	1.7	0.36	13	0.1	10.5	3.2	6.12	1.86	0.26	0.26	0.15	9.4	<5.00
KH-38	20.8	1.64	1.2	0.42	1.62	0.35	14	0.1	10	2.9	6.65	1.65	0.35	0.27	0.17	10	<5.00
KH-39	21.9	1.58	1.2	0.4	1.62	0.37	14	0.11	10.4	3	6.95	1.8	0.39	0.24	0.16	11	<5.00

**Table 4:** Results from study of rare earth elements in area.

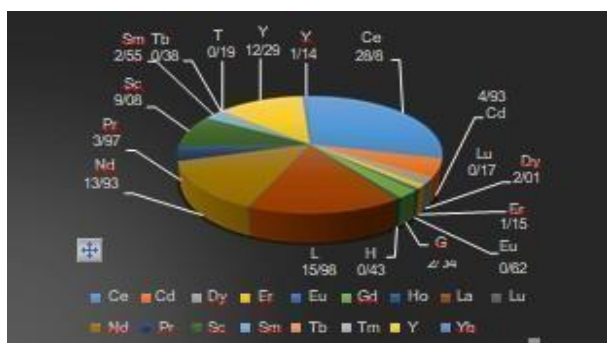


**Figure 4:** Average frequency percentage of rare earth elements in study areas.

### Discussion of geochemical results

**Study of main elements based on aluminum scale:** During the diagnosis, weathering and metamorphism, aluminum oxide is considered a constant factor [4], which is used as a scale in the study of the main elements of Clastic sediment.

However, CaO, Na<sub>2</sub>O and K<sub>2</sub>O are known as the most mobile phases in sandstones. The average percentage of aluminum oxide in the studied samples of regional sediments is about 11.35%. As can be seen in Figure 5, aluminum oxide shows a positive trend with oxides of K<sub>2</sub>O, MgO, TiO<sub>2</sub>, a positive trend with Fe<sub>2</sub>O<sub>3</sub>, and a negative correlation with CaO oxide in these areas.



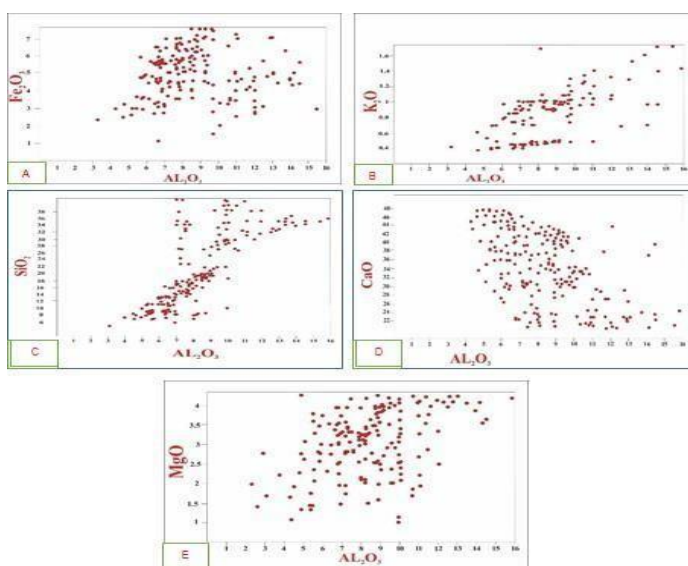


**Figure 5:** Investigation of changes in main oxides with aluminum oxide. A) Positive relationship between  $Al_2O_3$  and  $Fe_2O_3$ , B) Positive relationship between  $Al_2O_3$  and  $K_2O$ , C)

Positive relationship between  $Al_2O_3$  and  $SiO_2$ , D) Negative relationship between  $Al_2O_3$  and  $CaO$ , E) Positive relationship between  $Al_2O_3$  and  $MgO$ . The changes of two  $TiO_2$  with  $Al_2O_3$  oxides show that they have a positive trend towards each other (Figure 6(A)). The average percentage of  $TiO_2$  oxide in the area is 0.7%. The element titanium is more concentrated in phyllosilicates and is a good indicator for interpreting the source rock due to the immobility during the sedimentary processes compared to other elements [5]. The increase of  $Al_2O_3$  together with  $TiO_2$  indicates the association of  $TiO_2$  with phyllosilicates in these areas.

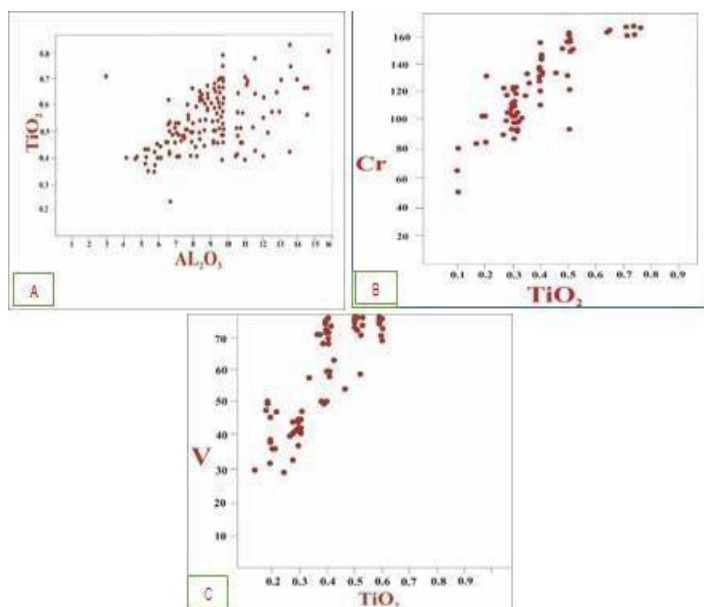


**Figure 6:** Relationship between Titanium Oxide ( $TiO_2$ ) and Aluminum Oxide ( $Al_2O_3$ ) and elements Vanadium (V) and chromium; A) positive relationship between  $TiO_2$  and  $Al_2O_3$ , B) positive relationship between  $TiO_2$  and Cr, C) Positive relationship between  $TiO_2$  and V. Also, the study of changes in elements V and Cr with titanium oxide shows a positive relationship between this oxide and the mentioned elements (Figure 6(B, C)). Since Cr and V are associated with iron and titanium in heavy minerals, the correlation of Cr and V with  $TiO_2$  oxide indicates the presence of heavy minerals in the areas. In the study area, the petrographic data confirm the existence of heavy minerals [6].

The same correlation trend can be observed in the comparison of aluminum oxide  $Al_2O_3$  with Scandium (Sc), Vanadium (V), Thorium (Th), Cobalt (Co), Niobium (Nb), Chromium (Cr), and Lanthanum (La) (Figure 7). One of the reasons for the presence of heavy minerals is the positive correlation between these elements, especially  $Al_2O_3$  and Cr, in the areas. The presence of the heavy elements has been identified in petrographic studies.

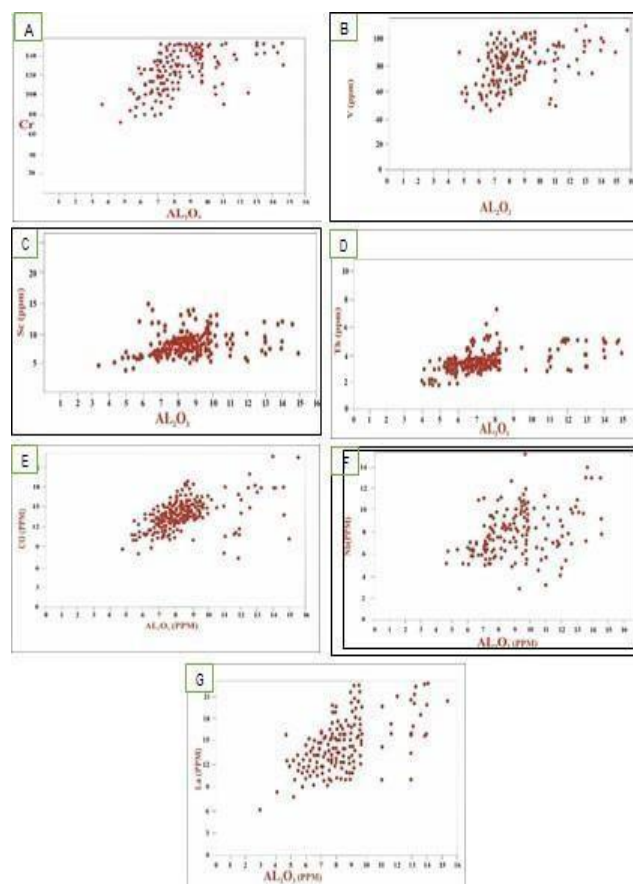


**Figure 7:** Relationship between aluminum oxide and sub- elements. A) Positive relationship between  $Al_2O_3$  and Cr, B) Positive relationship between  $Al_2O_3$  and V, C) Positive relationship between  $Al_2O_3$  and Sc, D) Positive relationship between  $Al_2O_3$  and Th, E) Positive relationship between  $Al_2O_3$  and Co, F) Positive relationship between  $Al_2O_3$  and Nb, G) Positive association between  $Al_2O_3$  and La.

**Geochemical classification of sediments:** Apart from using petrographic methods, researchers use a combination of main elements in the classification and the separation of mature and immature sediments [7]. Geochemical classification of sandstones based on the log (Fe<sub>2</sub>O<sub>3</sub>/K<sub>2</sub>O) vs log (SiO<sub>2</sub>/Al<sub>2</sub>O<sub>3</sub>) diagram is used to classify sandstones [8]. Most of the samples studied in the plotted diagram are among ferruginous shales (Figure 8).

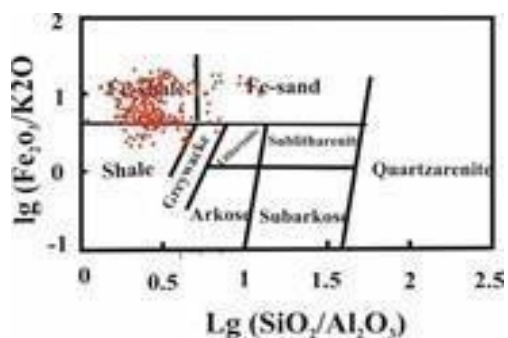


**Figure 8:** Classification of sand samples studied in diagram.

Geochemical classification of sandstones based on the classification of clastic sandstones, which is based on chemical maturity indices. According to this diagram, most of the samples in the area have a greywacke composition, which is consistent with the petrographic data (Figure 9).

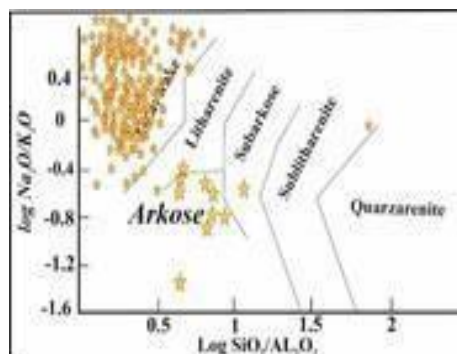


**Figure 9:** Geochemical classification of samples studied on diagram.

**Studies of primary weathering of sediments:**

In the study of sandstones that have not been strongly affected by diagenesis and metamorphism or other alteration and weathering processes, the geochemical analysis of the main elements of clastic rocks is a suitable tool for determining the tectonic setting [9]. The Chemical Index of Alteration (CIA) has the most application in the relation proposed by [10]. This index is obtained by the following formula where oxides are expressed in molar ratio.

$$CIA = (Al_2O_3 / (Al_2O_3 + CaO^* + Na_2O + K_2O)) \times 100$$

The average of this index for 276 samples studied in the area is 19.97, which indicates the hot arid climate conditions of the source area.

Elements	CIA	Elements	CIA
<b>Sample No</b>		<b>Sample No</b>	
D-2	18/64	D-33	12/68
D-3	18/53	D-34	13/82
D-4	27/54	D-35	16/30
D-5	18/96	D-36	15/37
D-8	18/55	D-37	10-Oct
D-11	16/93	D-38	17/8
D-12	18/84	D-39	13/75
D-13	16/37	D-40	17/61
D-14	13/49	D-43	13/71
D-16	12/73	D-44	14/89
D-17	03/4	D-45	13/53
D-18	16/16	D-46	17/68
D-20	15/71	D-47	13/21
D-23	17/6	D-49	15/23
D-24	14/70	D-53	11/32
D-25	12/25	D-54	12/77

D-26	13/64	D-56	9/40
D-27	13/71	D-57	15/89
D-28	11/34	D-58	15/75
D-29	10/53	D-59	12/70
D-30	12/77	D-60	13/14
D-31	15/45	D-61	14/7

**Table 5:** Average CIA index in study areas. Presented another weathering index for sandstones with variable amounts of CaO. This index is defined as follows:

$$CIW = (Al_2O_3 / (Al_2O_3 + Na_2O)) \times 100$$

The results of this index were obtained, on average, equal to 82.66 for the samples of the area. This value indicates the long distance

sediment transport from the origin to the sedimentation area and the hot arid climate of the source area for the samples (Table 6).

Elements	CIW	Elements	CIW
Sample No		Sample No	
D-2	70/43	D-34	72/65
D-3	75/10	D-35	69/89
D-4	75/63	D-36	95/46
D-5	76/02	D-37	59/74
D-8	84/15	D-38	84/21
D-11	83/13	D-39	77/43
D-12	86/21	D-40	70/67
D-13	66/79	D-43	86/27
D-14	78/38	D-44	86/90
D-16	81/84	D-45	78/00
D-17	89/36	D-46	91/74
D-18	93/64	D-47	76/25
D-20	91/42	D-49	84/76
D-23	85/02	D-53	75/70
D-24	81/09	D-54	76/59
D-25	67/95	D-56	86/29
D-26	81/67	D-57	81/16
D-27	68/22	D-58	80/47
D-28	81/25	D-59	76/45
D-29	75/44	D-60	87/02
D-30	68/73	D-61	83/70
D-31	77/29	D-63	74/71
D-33	75/17	D-64	76/83

**Table 6:** Average CIW index in study areas.



The moderate weathering obtained for the samples may indicate the intense activity of the sediment recycling in semi-humid climates or the presence of recycling in semi-arid to arid climates. In addition, from the A-CN-K diagram, the weathering path can be obtained from both weathering profile method and thermodynamic estimation method.

Plotting the samples in this diagram shows that the data are close or parallel to the A-CN line. Plotting the samples in this diagram shows that the samples area do not show the dispersion and a wide range relative to the line connecting the feldspars in the diagram (Figure 10), which indicates the severe chemical weathering or the presence of recycling in clastic sediments.

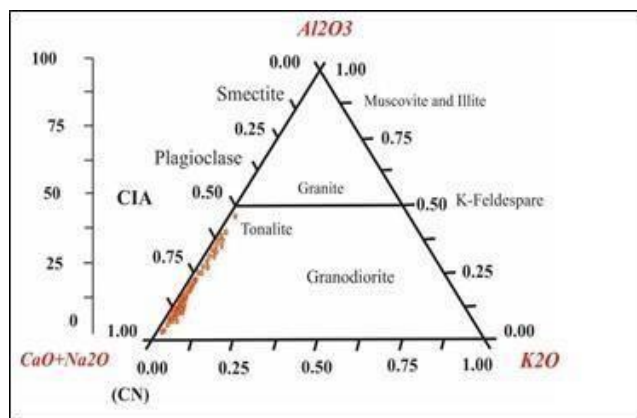


**Figure 10:** Plotting samples of study areas in combined space of A-CN-K diagram and its amount relative to line connecting feldspars. In the source area, the paleoclimate conditions can be predicted by plotting the diagram of  $\text{SiO}_2$  against  $\text{Al}_2\text{O}_3 + \text{K}_2\text{O} + \text{Na}_2\text{O}$ . According to this diagram (Figure 11), the paleoclimate in the source area during the sedimentation in the study area was arid to semi-arid climate. These results are completely consistent with those obtained from the diagram [12].

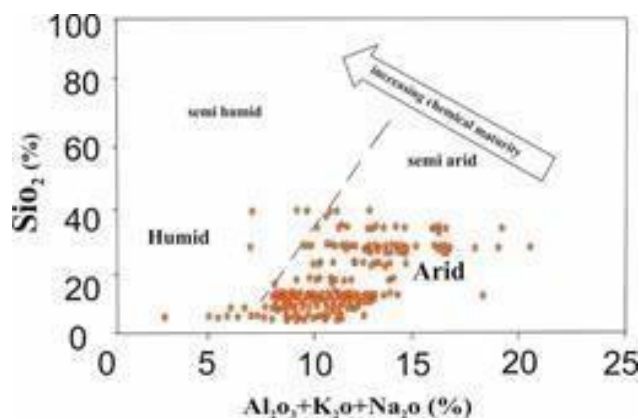


**Figure 11:** Diagram for determination of paleo climate conditions in area based on diagram.

**Determination of tectonic setting of sediments:** The Clastic sediments of oceanic island arcs, continental island arcs, active continental margin, and passive margin can be distinguished by changing the values of the main elements. Using the diagram to determine the tectonic setting of the studied sediments, it is found that the samples of this area are mainly present in the active continental margin (Figure 12) [11].

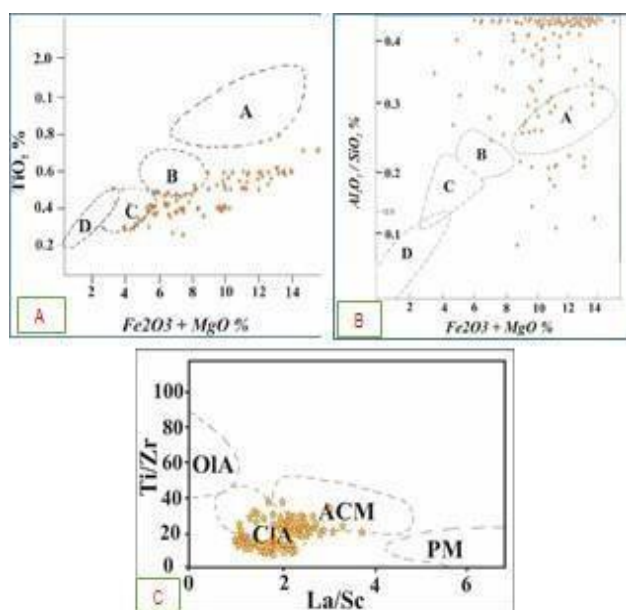


**Figure 12:** Determination of tectonic setting of sediments; A) diagram of composition of main elements on Bahatia's diagram based on  $\text{TiO}_2$  index vs  $\text{Fe}_2\text{O}_3 + \text{MgO}$ , B) separating diagram based on ratio of  $\text{Al}_2\text{O}_3/\text{SiO}_2$  vs  $\text{Fe}_2\text{O}_3 + \text{MgO}$  according to diagram. C) Plotting composition of sub-elements of clastic sediments in area on tectonic setting diagram based on  $\text{La}/\text{Sc}$  index against  $\text{Ti}/\text{Zr}$ . A=OIA: Oceanic Island Arc, B=CIA: Continental Island Arc, C=ACM: Active Continental Margin, D=PM: Passive continental Margin. In addition to the presented diagrams, to determine the tectonic setting of the clastic samples of the area, the diagram of was used based on sub-elements. As can be seen from this diagram (Figure 13(A)) reviewing the diagram of [13] identified the geological setting of the active continental margin for the samples in the study area (Figure 13(B)).

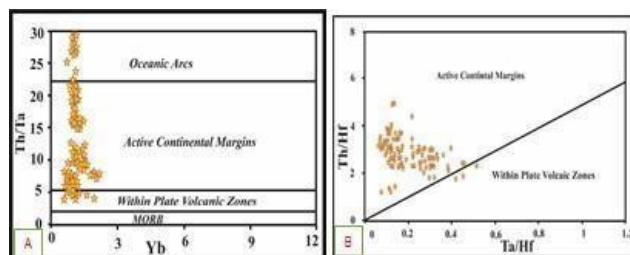


**Figure 13:** Determination of tectonic setting of sediments in area based on diagrams. A) Determination of tectonic setting based on ratio of  $\text{Th}/\text{Ta}$  to  $\text{Yb}$  in study areas based on diagram. B) Diagram for determination of tectonic setting based on ratio  $\text{Th}/\text{Hf}$  to  $\text{Ta}/\text{Hf}$  in study areas.

**Ratios of main elements in relation to source rock:** The clastic sediments of oceanic island arcs, which are derived from calc-alkaline andesites, have higher levels of  $\text{Na}_2\text{O}$ ,  $\text{Al}_2\text{O}_3$ ,  $\text{TiO}_2$  and  $\text{Fe}_2\text{O}_3$  and relatively lower levels of  $\text{SiO}_2$  and  $\text{K}_2\text{O}$ , which distinguishes them from other sedimentary samples. In addition, from the determination of the source rock of sediments using main and sub-elements, the felsic source rock contains higher values of Sr and Ba and lower values of Ni, Co, Cr, V compared to mafic source rock [14].

The increases of Ni, Co, Cr, V along with MgO in the studied samples indicate the mafic source of the sediments [15]. As can be seen in Figures 14(A-D), most of the samples have a felsic source and some of the samples have a mafic source, which indicates the transport of sediments from both sources to the mentioned areas (Figure 14).

In the diagram (Figure 14(A)), the coherent increase in the percentages of V and MgO indicates the mafic source of the sediments. The increasing trend in the frequency of Cr and MgO indicates the mafic source of the sediments (Figure 14(B)). On the other hand, the coherent mutual increase of Co with MgO indicates the mafic source of the sediments (Figure 14(C)). Finally, the frequency of Ni along with MgO also indicates the mafic source of the sediments in the study areas (Figure 14(D)).

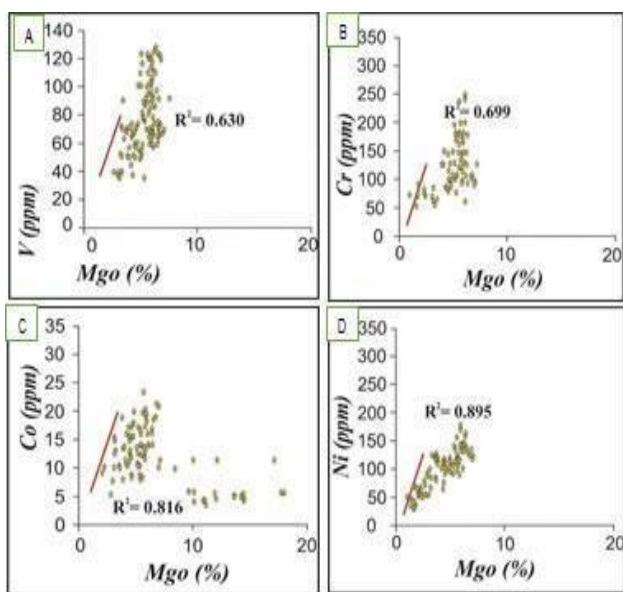


**Figure 14:** Ratios of main elements in relation to tectonic setting in area based on diagram.

A) Relationship between percentage of magnesium oxide and sub-element V, B) Relationship between percentage of magnesium oxide and sub-element Cr, C) Relationship between percentage of magnesium oxide and sub-element Co, D) Relationship between percentage of magnesium oxide and sub-element Ni. Using the diagrams obtained from plotting  $\text{TiO}_2$  vs Zr, the basic source rock can be distinguished from the intermediate and felsic limits (Figure 15(A)). In acidic rocks, sub-elements such as Nb, Zr, Hf, Th and La are more frequent, and in mafic rocks, elements such as Ni, Cr, Co, Sc are more frequent. These elements to separate source rock (Figure 15(B)). On the other hand, diagrams of Cr/V vs Y/Ni and La/Th vs Hf are used to identify source rock (Figure 15(C)).

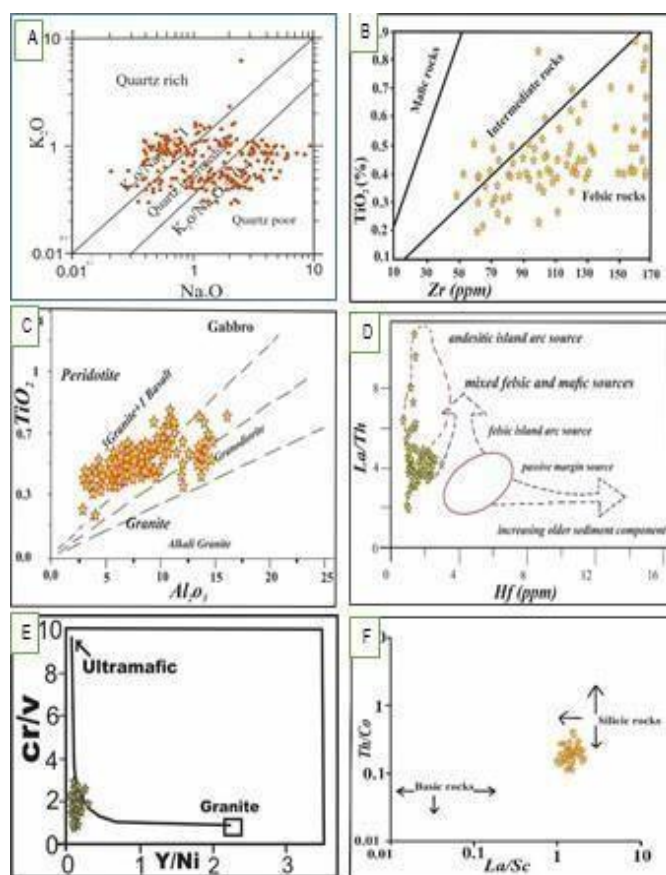


**Figure 15:** Determination of source rock of sediments in study areas; A) Determination of source composition based on  $\text{Na}_2\text{O}$ - $\text{K}_2\text{O}$  diagram in studied sediments, B) Plotting values of studied samples on  $\text{TiO}_2$  and Zr diagrams of  $\text{Al}_2\text{O}_3$  vs  $\text{TiO}_2$  to determine source of studied sediments based on diagram. C) In addition, the La/Th vs Hf diagram was used for the source rock composition of sediments in the study areas. D) Plotting values of trace elements for studied samples. E) As shown in diagram of La/Th vs Plotting sub-element values of studied samples on diagram of Cr/V vs Y/Ni, F) Source rock composition of studied samples on diagram of Th/Co vs La/Sc.

As shown in Figure 15(A), the amount of  $\text{TiO}_2$  in the area varies between 0.19 and 0.91%, while the amount of Zr in this area generally varies between 56.4 and 273.4 ppm (Figure 15(A)). According to this diagram, the sediments in the area are probably of felsic source. The samples are of siliceous source in the Th/Co vs La/Sc diagram (Figure 15(B)) in this study area. In addition, the La/Th vs Hf diagram was used for the source rock composition of sediments in the study areas (Figure 15(C)). Based on this diagram, it can be concluded that felsic source rock can be suggested for the sediments of the area.

### Mineralogical studies

The mineralogical studies by X-Ray Diffraction (XRD) along with the geochemical studies show very good information about the mineralogical properties of the studied sediments. In these studies, 276 samples of the area were analyzed using XRD (Table 7).

No	Origin	Main mineral phase	Sub-mineral phase	Rare mineral phase
1	Domestic	Calcite, Quartz, Halite	Albite, Gypsum, Dolomite, Chlorite, Illite	–
2	Domestic	Calcite, Quartz, Halite, Dolomite	Albite, Gypsum, Chlorite, Muscovite	–
3	Domestic	Calcite, Quartz, Halite	Albite, Gypsum, Chlorite, Illite	Dolomite
4	Foreign	Calcite, Halite	Albite, Dolomite, Chlorite, Quartz	Gypsum, Illite
5	Foreign	Calcite, Quartz, Halite, Dolomite	Albite, Chlorite, Illite	–
6	Foreign	Calcite, Quartz, Albite, Dolomite	Illite	Chlorite, Halite, Orthoclase
7	Foreign	Calcite, Quartz	Illite, Albite, Dolomite, Halite	Chlorite, Gypsum
8	Domestic	Calcite, Quartz	Illite, Albite, Dolomite, Hematite	–
9	Domestic	Calcite, Quartz, Halite	Illite, Albite, Dolomite, Chlorite	–
10	Domestic	Calcite, Quartz, Halite	Illite, Albite, Dolomite, Chlorite	–
11	Foreign	Calcite, Quartz, Dolomite	Chlorite, Albite, Halite, Gypsum	–

**Table 7:** Sample of mineralogical studies performed on some samples. The data from these studies show that calcite, quartz, dolomite and halite are the most frequent minerals in the studied deposits. In this area, albite, gypsum, chlorite and illite are among the sub-minerals in these deposits (Figures 16-20).

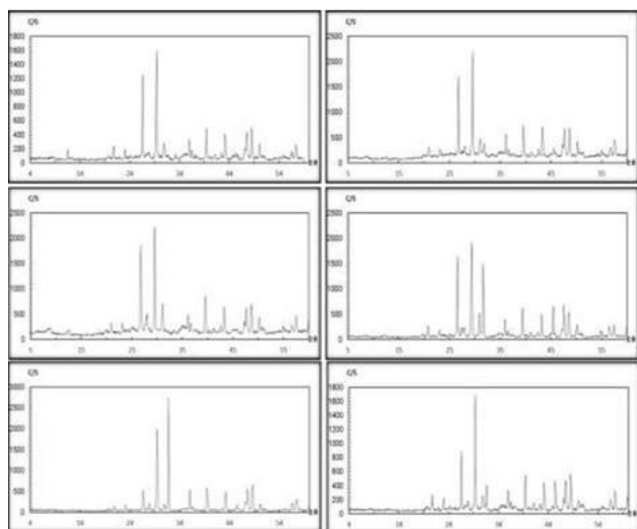


**Figure 16:** X-ray diffraction pattern of some studied samples.

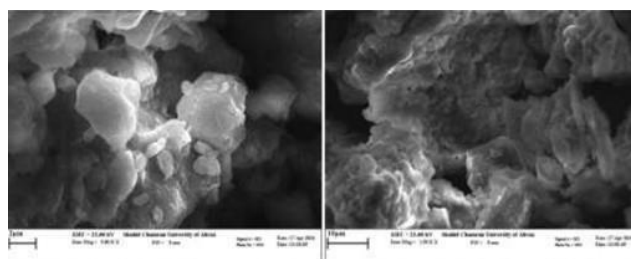


**Figure 17:** Electron microscopy images of studied calcite samples.

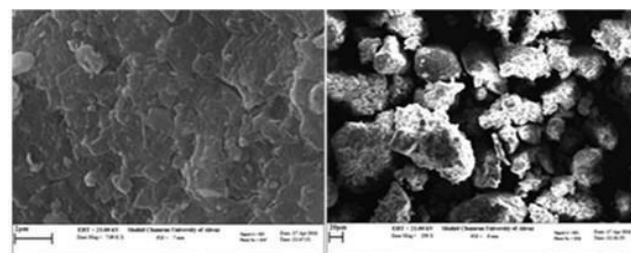


**Figure 18:** Electron microscopy images of studied clay samples.

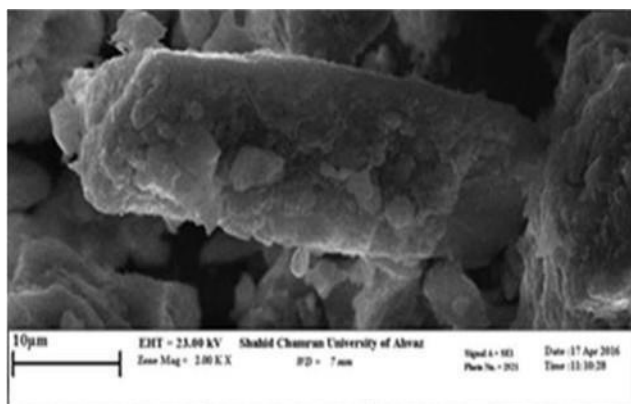


Figure 19: Electron microscopy images of studied evaporate samples.

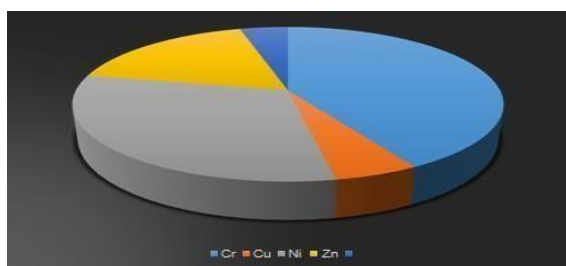


Figure 20: Frequency of heavy metals in study areas (%).

## Environmental properties

In the comprehensive study of sediments in the area, the accurate environmental studies are necessary, especially in places close to residential areas.

## Environmental contamination

**Study of heavy metals:** One of the most important environmental contaminants is soil contamination with heavy metals. In terms of toxicity and stability, they are one of the most dangerous groups of contaminants, and due to the soil contamination characteristics, the accumulation in tissues of living organisms, long lifespan, and toxicity are of great ecological and biological importance [16].

In these studies, 276 samples of sediments in the area were examined and evaluated (Tables 8). According to the studies, the average frequency of the metals in the area in order of frequency include Zn with a frequency of 48.86 ppm, Pb with a frequency of 31.25 ppm, Cu with a frequency of 15.75 ppm, and Cd with a frequency of 4.12 ppm (Figure 20).

**Discussion of contamination indicators:** As can be seen from the data obtained from the average contamination caused by different elements (Table 8), the area has moderate contamination in terms of Zn, Ni and V elements.

Sample No	Elements				
	Cr	Cu	Ni	Zn	Co
D-2	92/5	21/2	114	49/4	12/8
D-3	133	20/4	143	68/7	16/3
D-4	131	19/0	124	55/3	14/9
D-5	114	30/5	121	57/7	15/9
D-8	161	27/2	156	67/5	18/5
D-11	120	26/2	115	60/1	14/9
D-12	148	20/5	136	56/7	16/4
D-13	115	17/6	114	50/7	14/2
D-14	109	16/3	92	45/0	12/8
D-16	121	21/2	105	86/3	14/8
D-17	135	28/7	118	61/4	16/0
D-18	138	18/4	109	55/6	15/8

Table 8: Results obtained regarding amount of CF in area.



The results of the Contamination Factor (CF) method for the study of 276 samples in the study area are somewhat similar to the results of the method of the contamination calculation and indicate that in the area. These contaminants are probably caused by drilling fluids or oil leakage through the joints and fissures of the cap rock to the upper parts in the upstream of this area (Figure 2.6) [17].

## Conclusion

The most important results are summarized as follows. The results of granulometric studies indicate that the sediments are mainly of silt and clay size, and the particles of sand and gravel size are less frequent in the study areas. The study of geochemical properties of the sediments indicates that the most frequent constituent oxides in the study area are Cao, SiO<sub>2</sub> and Al<sub>2</sub>O<sub>3</sub>, respectively. The results of the studies show that calcite, quartz, dolomite and halite are the most frequent minerals in the studied deposits. In this area, albite, gypsum, chlorite and illite are among the sub-minerals in the deposits.

According to the studies, the most frequent sub-elements in the study areas are Ti, Zr, V, Ce and La, respectively. The classification of sediments based on the geochemical indicators shows that the sediments are mainly in the range of greywacke and ferruginous shale. In addition, the study of pale climate conditions indicates the arid to semi-arid climate in the source area of the sediments. The study of the tectonic setting in the study area based on the geochemical properties of the mentioned sediments indicates the tectonic settings of continental island arc and active continental margin. The routing of the mentioned sediments indicates the mainly felsic and sometimes mafic source of the sediments. The study of environmental contamination in the study areas indicates that the elements Ni, Cr and Zn are the most frequent heavy metals in the sediments.

## References

1. Alavi M (2007) Structures of the Zagros fold-thrust belt in Iran. *Am J Sci* 307: 1064-1095.
2. Adabi MH, Kakemem U, Sadeghi A (2016) Sedimentary facies, depositional environment, and sequence stratigraphy of Oligocene-Miocene shallow water carbonate from the Rig Mountain, Zagros basin (SW Iran). *Carbonates Evaporates* 31: 69-85.
3. Zakeri M, Grutzner C, Navabpour P, Ustaszewski K (2019) Relative timing of uplift along the Zagros Mountain Front Flexure (Kurdistan Region of Iraq): Constrained by geomorphic indices and landscape evolution modeling. *Solid Earth* 10: 663-682.
4. Shoorangiz M, Sarkarinejad K, Nourbakhsh A (2020) Tectonic implication of quantitative micro-fabric analyses of quartz c-axis development within the Tutak gneiss dome, Zagros hinterland fold-and-thrust belt. *Int J Earth Sci* 109: 1-18.
5. Karasozen E, Nissen E, Bergman EA, Ghods A (2019) Seismotectonics of the Zagros (Iran) from orogeny wide, calibrated earthquake relocations. *J Geophys Res Solid Earth* 124: 919-929.
6. Heidari A, Raheb A (2020) Geochemical indices of soil development in arid to sub-humid climosequence of Central Iran. *J Mt Sci India* 17: 1652-1669.
7. Smirnov PV, Konstantinov AO, Aleksandrova GN, Kuzmina OB, Shurygin BN (2019) New data on the lithology of coastal facies of the Turtas Formation (Upper Oligocene, Southwestern Siberia). *Dokl Earth Sci* 475: 868-871.
8. Sharma RP, Raja P, Bhaskar BP (2020) Pedogenesis and mineralogy of alluvial soils from semi-arid southeastern part of Rajasthan in Aravalli Range, India. *J Geol Soc India* 95: 59-66.
9. Ho Thi P, Kenji O, Md AU (2019) Geochemistry and sediment in the main stream of the Ca River basin, Vietnam: weathering process, solute-discharge relationships and reservoir impact. *Acta Geochim* 38: 627-641.
10. Al Hashim MH, Herron PL (2020) Geochemistry of the Paleoproterozoic Espanola Formation, Bruce Mines-Elliot Lake area, Ontario, Canada: Implications for provenance, paleo weathering, and tectonic setting. *Geosci J* 25: 125-144.
11. Oreshkina TV, Aleksandrova GN, Lyapunov SM (2020) Micropaleontological and lithochemical characteristic of the Turtas Formation, Western Siberia. *Stratigr Geol Correl* 28: 311-329.
12. Nesbitt HW, Young GM (1982) Early Proterozoic climates and plate motions inferred from major element chemistry of lutite. *Nature* 299: 715-717.
13. Abu M, Sunkari ED, Gurel G (2020) Paleocurrent analysis, petrographic, geochemical and statistical appraisal of neoproterozoic siliciclastic sediments, NE voltaian basin, Ghana: A multidisciplinary approach to paleogeographic reconstruction. *J Sediment Environ* 5: 199-218.
14. Paikaray S, Banerjee S, Mukherji S (2008) Geochemistry of shales from the Paleoproterozoic to Neoproterozoic Vindhyan Supergroup: Implications on provenance, tectonics and paleoweathering. *J Asian Earth Sci* 32: 34-48.
15. Bhatia MR (1986) Trace element characteristics of greywakes and tectonic setting discrimination of sedimentary basins. *Contrib to Mineral Petrol* 92: 181-193.
16. Schandl ES, Gorton MP (2002) Application of high field strength elements to discriminate tectonic setting in VMS environment. *Econ Geol* 97: 629- 642.
17. Roser BP, Korsch RJ (1988) Provenance signatures sandstone-mudstone suites determined using discriminate function analysis of major element data. *Chem Geol* 67: 119-139.